

# Thermoacoustic Analysis of Combustion Instability Importing RANS Data

Giovanni Campa<sup>\*1</sup>, E. Cosatto<sup>2</sup>, S.M. Camporeale<sup>1</sup>

<sup>1</sup>Politecnico di Bari, <sup>2</sup>Ansaldo Energia, Genova

\*DMMM – Sez. Macchine ed Energetica – Politecnico di Bari – via Re David 200, 70125 Bari, Italy  
campa@imedado.poliba.it

**Abstract:** Thermoacoustic combustion instabilities affect modern gas turbines equipped with lean premixed dry low emission combustion systems. A hybrid technique based on the use of the finite elements method and the transfer matrix method is used to identify the frequencies at which thermoacoustic instabilities are expected and the growth rate of the pressure oscillations at the onset of instability, under the hypothesis of linear behavior of the acoustic waves. The Helmholtz equation is used to model the combustion chamber and the classical  $\kappa$ - $\tau$  formulation for the flame model is adopted. The gas turbine combustion chamber by Ansaldo Energia is modeled in COMSOL Multiphysics. Operating conditions are taken from experimental data and from Reynolds Averaged Navier Stokes (RANS) simulations of Ansaldo combustor. File data from RANS simulations are therefore imported into COMSOL. The proposed method is therefore able to establish a theoretical relation of the characteristics of the flame to the onset of the thermoacoustic instability.

**Keywords:** Import Data File, Transfer Matrix Method, Thermoacoustics, Burners, Eigenvalues.

## 1. Introduction

The introduction of lean premixed burners in gas turbine systems for power generation has determined an increase of the risk of thermoacoustic instabilities [1][2][3]. This phenomenon is caused by self-sustained pressure oscillations, which arise from coupling of heat release fluctuations and acoustic waves propagating within the combustion system. These instabilities are dangerous because can lead to strong vibrations of the system with consequent structural damages. The phenomenon is known since a long time and several models and techniques have been proposed over the years to have a better comprehension of its causes and to predict which operating conditions are more prone to cause it.

Quite often low-order models [4][5][6][7] are proposed to represent the combustion instability in the combustion system modeled as a network of acoustic elements (and so the name of Acoustic Networks), where each element corresponds to a component, such as a duct, a nozzle, a burner. Generally, each component represents a one-dimensional propagation of the acoustic waves, mainly within the limits of the linear acoustic and harmonic time dependence ( $i\omega t$ ). These tools may be used to study the pressure oscillations by dividing the combustor into a series of subsystems, using mathematical transfer function matrices to connect these lumped acoustic elements one to each other, so providing the continuity of acoustic velocity and pressure across each zone. These models are very helpful to understand the instability mechanisms, but when complex three-dimensional geometries are involved, these models become unable to model the propagation of the acoustic waves adequately.

LES (Large Eddy Simulation) codes are proposed by several authors [8][9][10][11] to investigate the phenomenon of combustion instability and matching pressure oscillations with turbulent combustion phenomena, considering the dynamically relevant scales during the resolution, related to fluid dynamic phenomena and the kinetic chemistry. The disadvantages are concerned with the enormous computational efforts required for the resolution.

A finite element method (FEM) approach may also be used to solve the acoustic problem in three-dimensional geometries [12][13][14][15]. The differential equation problem converted in a complex eigenvalue problem in the frequency domain is solved and complex eigenfrequencies of the system are detected to ascertain if the corresponding modes are stable or unstable [14][15].

In this paper a hybrid technique is described, since the combination of lumped elements and three-dimensional elements is achieved. The numerical procedure, able to detect the complex eigenvalues of the analyzed system in presence

of a flame transfer function and a transfer matrix function, is implemented in COMSOL. Each burner is described not as a computational domain, but as a mathematical function, using the transfer matrices of the low-order models [16]. Data from RANS simulations are used to obtain a distribution of the Flame Response Function (FRF) of the  $\kappa$ - $\tau$  type as a function of the position within the chamber. RANS data are properly modified in the grid format to be imported in COMSOL and to match the two different computational grids (the RANS one and the COMSOL one).

## 2. Mathematical Model

As regards gas turbine combustion systems, the flow velocity is generally far below the sound velocity, both in the plenum placed at the exit of the compressor and in the combustion chamber, while the flow velocity is not negligible in some limited areas, such as conduits of single burner or multiple burners that connect the plenum to the chamber. These areas, in terms of propagation of pressure waves, can be treated as “compact” elements that can be modeled by means of specific transfer function matrices, obtained experimentally or numerically through CFD or aeroacoustics codes. The hybrid method proposed here makes a combined use of FEM, for the analysis of the propagation of the acoustic wave in 3D domains with negligible flow velocity, and transfer matrices to model the acoustic waves in the ducts of the burners, where there is a one-dimensional propagation of the waves, in presence of not negligible levels of flow velocity.

In the acoustic analysis each variable is assumed to be composed of a steady mean value (identified by an overbar) and a small perturbation (identified by a prime):  $p(\mathbf{x},t) = \bar{p}(\mathbf{x}) + p'(\mathbf{x},t)$  and  $\mathbf{u}(\mathbf{x},t) = \bar{\mathbf{u}}(\mathbf{x}) + \mathbf{u}'(\mathbf{x},t)$ . The flow velocity is considered negligible in comparison with the sound velocity, within the computational domain, so  $\bar{\mathbf{u}}(\mathbf{x}) = 0$  in the whole domain. The effects of viscous losses and thermal diffusivity can also be neglected, while the temperature can vary within the domain under the simplifying hypothesis that the fluid can be considered as an ideal gas, which means that specific heats are supposed constant and the variation of the composition caused by combustion does not

produce a variation of the number of moles. From these hypotheses, in presence of heat fluctuations, the linearized equations for the perturbations can be obtained [17][18], giving the inhomogeneous wave equation

$$\frac{1}{\bar{c}^2} \frac{\partial^2 p'}{\partial t^2} - \bar{\rho} \nabla \cdot \left( \frac{1}{\bar{\rho}} \nabla p' \right) = \frac{\gamma-1}{\bar{c}^2} \frac{\partial q'}{\partial t} \quad (1)$$

where  $c$  is the speed of sound and  $q'$  is the fluctuation of the heat input per unit volume. The term at the RHS of Eq.(1) shows that the rate of non-stationary heat release creates a monopole source of acoustic pressure disturbance. Considering that mean flow velocity is neglected, no entropy wave is generated and the pressure fluctuations are related to the velocity fluctuations by

$$\frac{\partial \mathbf{u}'}{\partial t} + \frac{1}{\bar{\rho}} \nabla p' = 0. \quad (2)$$

This work is conducted in the frequency domain, so that each variable fluctuation is expressed as a complex function of time:

$$p' = \text{Re}(\hat{p}(\mathbf{x}) \exp(i\omega t)) \quad (3)$$

where the hat refers to a complex variable and the same is for the other variables. Introducing this condition into Eq.(1), the Helmholtz equation can be obtained:

$$\frac{\lambda^2}{\bar{c}^2} \hat{p} - \bar{\rho} \nabla \cdot \left( \frac{1}{\bar{\rho}} \nabla \hat{p} \right) = -\frac{\gamma-1}{\bar{c}^2} \lambda \hat{q} \quad (4)$$

where  $\lambda = -i\omega$  is the eigenvalue, being  $\omega$  a complex variable, comprising a real part that gives the frequency of oscillations and an imaginary part that gives the growth rate at which the amplitude of oscillations increases per cycle. Eq.(4) shows a quadratic eigenvalue problem which can be solved by means of an iterative linearization procedure. COMSOL Multiphysics uses the Arpack Fortran as numerical routines for large-scale eigenvalue problems. It is based on a variant of the Arnoldi algorithm, called the implicit restarted Arnoldi method [19]. An iterative procedure based on a quadratic approximation around an eigenvalue linearization point  $\lambda_0$  is adopted. Such a procedure is speeded up by using, as approximate starting eigenvalue, the value

obtained through the analysis of the system without heat release fluctuations. The solver reformulates the quadratic eigenvalue problem as a linear eigenvalue problem of the conventional form  $Ax = \lambda Bx$ , and, iteratively, updates the linearization point until the convergence is reached. The software approximates the nonlinear model with a linear model, and the approximation is valid only when the solution is close to the linearization point. This means that not always the obtained solution is the exact solution, but it could be a spurious solution, so that a manual re-initialization is needed.

## 2.1 Transfer Matrix Method

The transfer matrix is a 2x2 matrix whose coefficients can relate the fluctuations of acoustic pressure  $p'$  and velocity  $u'$  at one junction, or port of the element, to the fluctuations of acoustic pressure and velocity on the other junction of the element. In this work the burner is modeled by means of the transfer matrix proposed both by Fanaca [20] and Alemela [21] in order to model the burner used during their experiments at Technische Universitet of Munich. The transfer matrix is obtained assuming one-dimensional flow with low Mach number within a "compact element" represented by a duct having short length (compared to the wavelength), variable cross section and pressure losses. Linearizing the mass and momentum conservation equations, the following equations can be obtained

$$\left[ A \left( \frac{\hat{p}}{\rho c} M + \hat{u} \right) \right]_d^u = 0 \quad (5)$$

$$\frac{i\omega}{c} \hat{u}_u l_{eff} + \left[ M \hat{u} + \frac{\hat{p}}{\rho c} \right]_u^d + \zeta M_d \hat{u}_d = 0 \quad (6)$$

where  $M$  is the Mach number. In Eq.(6) the effective length  $l_{eff}$  given by

$$l_{eff} = \int_{x_u}^{x_d} \frac{A_u}{A(x)} dx, \quad (7)$$

takes into account the inertia of the air mass in the duct, assuming that the Mach number is sufficiently low and that the effect of air compressibility can be neglected. The coefficient  $\zeta$  gives the acoustical pressure losses and is

generally close to the mean flow pressure loss coefficient, due to friction and flow separation  $\zeta = 2\Delta p / (\bar{\rho} \bar{u}^2)$ . Using effective length  $l_{eff}$  and pressure loss coefficient  $\zeta$ , neglecting higher order Mach number terms, the transfer matrix of a compact element is obtained from Eq.(5) and Eq.(6)

$$\begin{bmatrix} \hat{p} \\ \hat{u} \end{bmatrix}_d = \begin{bmatrix} 1 & M_u - \alpha M_d (1 + \zeta) - ik l_{eff} \\ \alpha M_u - M_d & \alpha + M_d ik l_{eff} \end{bmatrix} \begin{bmatrix} \hat{p} \\ \hat{u} \end{bmatrix}_u \quad (8)$$

where  $\alpha = A_u / A_d$  is the area ratio and  $k = \omega / c$  is the wave number.

## 2.2 Flame Response Function

In order to obtain a flame configuration as realistic as possible, flame data coming from steady flow RANS simulations are introduced into COMSOL framework. Flame front is described by means of data regarding *Rate of Reaction-1*, which is relative to a two step reaction between methane and air. Volumetric heat release fluctuations  $q'$  are modeled by means of the following procedure:

- $\bar{q} = 0$  and  $\hat{q} = 0$  when *Rate of Reaction* is lower than an inferior limit, which is properly defined;
- in the other points  $\bar{q} = 0$  (volumetric heat release  $[W/m^3]$ ) is calculated considering the Lower Heating Value  $[J/kmol]$ .

In LP gas turbines, the greatest influence on heat release fluctuations is due to the instantaneous fuel-air ratio, which is influenced by airstream velocity at the premixer location. Following this suggestion, heat release fluctuations are linearly related to the air velocity at the inlet of the combustion chamber with a time delay  $\tau$

$$\frac{q'(\mathbf{x})}{\bar{q}(\mathbf{x})} = -\kappa \frac{u_i'(t - \tau(\mathbf{x}))}{\bar{u}_i} \quad (9)$$

where subscript  $i$  corresponds to the position at which acoustic velocity inside heat release law is referred. Heat release is expressed as

$$\bar{q} = RR(\mathbf{x}) \cdot LHV \quad (10)$$

where  $RR$  represents the spatial distribution of *Rate of Reaction* [ $kmol/m^3s$ ],  $LHV$  is the Lower Heating Value [ $J/kmol$ ] of the fuel.

The volumetric heat release model defined in Eq.(10) is transferred into the governing equation, so that heat release law is applied inside the whole combustion chamber domain, and not in a specific thin domain at the beginning of the combustion chamber.

In a large part of the literature the time delay  $\tau$  in the flame model is regarded as a constant value. However, time delay in an actual flame differs from one point to another and even from one frequency to another, so that a spatial distribution,  $\tau(\mathbf{x})$ , is introduced. Using the RANS analysis of the combustion system, time for a particle to go from the burner exit to the flame front is calculated, Figure 1. The procedure to detect this distribution is roughly the same proposed by Krebs et al. [22] and called “flight time” method by Giaque et al. [10]. Additionally, the use of the results from steady-state CFD computations to obtain the distribution of time delays for the burner model is suggested by Paschereit et al. [23]: from the CFD analysis they obtain the maximum time delay and the time delay spread to be introduced into their flame transfer matrix. In this paper a spatial distribution for  $\tau$  is obtained by means of 4480 particles (35 times the number of particle injection points considered by [23]).

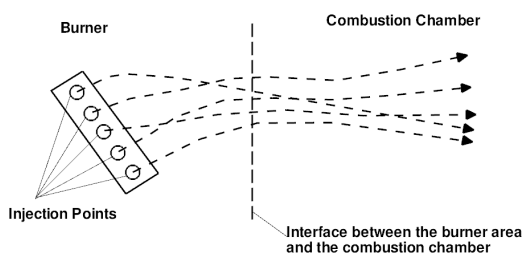


**Figure 1.** Sketch of one element of the injection system and the initial pathlines of the particles.

Each particle is followed from the injection point inside the burner until the flame front:

- For each particle the time taken to go from the injection point to the combustion chamber entrance (the motion inside the burner) is calculated, Figure 1.  $\tau_1$  is the

mean value among the values calculated in this way.

- For each particle the time inside the combustion chamber is calculated as the time taken to go from the combustion chamber entrance to the point on the flame front in which the *Rate of Reaction* is maximum. This time is  $\tau_2$ .
- The time delay for each particle is  $\tau = \tau_1 + \tau_2$  and it refers to the point along the pathline where the *Rate of Reaction* is maximum.

### 2.3 Boundary and Operating Conditions

The actual annular combustion chamber is modeled in COMSOL with its own 3D geometry. All the geometrical details smaller than the acoustic wavelength are removed in order to decrease the number of computational cells. Once a fine computational grid is realized, the operative and the boundary conditions are defined. The plenum is characterized by a uniform distribution of the main parameters. In particular, the temperature in the plenum is constant and its value is the one of the flow exiting the last stage of the axial compressor: it is a reasonable condition since the flow inside the plenum is mainly at the same temperature. On the other hand, the temperature inside the combustion chamber is not uniform, as usually it is assumed in the traditional models adopting the flame sheet concept. The temperature value changes cell by cell depending on the position inside the chamber and on position and shape of the flame. The thermal field inside the combustion chamber can be obtained by means of proper RANS data, as lately shown.

The definition of the boundary conditions is a very important step. The inlet and outlet boundary conditions are assumed to be close ends, meaning that the material derivative of the velocity fluctuations is set to be zero,  $u' = 0$ .

### 3. Use of COMSOL Multiphysics

In this work, the *Acoustic Module* is the COMSOL module which is used to perform the thermoacoustic analysis of the annular combustion chamber by Ansaldo Energia. The application mode *Pressure Acoustics* is used to solve the Helmholtz equation. The *Eigenfrequency* solver is used to identify the

complex eigenfrequencies of the combustor system.

The main point of this paper is the introduction of data coming from RANS simulations in the COMSOL model of the combustion chamber. RANS simulations of the combustor system were performed in Ansaldo Energia making use of ANSYS Fluent. Information about the temperature distribution and the flame behavior are taken from those simulations and transferred to the COMSOL model. In order to make possible this operation, the following procedure is adopted:

- data from Fluent are exported as a text file, since COMSOL imports text file as well, where each point of the computational grid is associated to the value of the chosen variable in that point;
- the format of the file data from Fluent is different from the format required by COMSOL, so that a manipulation of the file is needed. A routine (a Fortran routine in this work) is written for this purpose. Not only the format is modified, but also the point coordinates in order to have the correspondence between the computational grids;
- the modified file data are imported in COMSOL and used to describe some variables, such as the temperature.

#### 4. Application

An actual annular combustion chamber of a heavy duty gas turbine system produced by Ansaldo Energia [24] is examined. Following an approach tested in other works [25][26], only one quarter of the whole combustor is analyzed, applying symmetric conditions on periodic faces. In one quarter there are 6 burners, so that the BTM is applied 6 times. The geometry and the boundary conditions are shown in Figure 2 and the computational mesh is shown in Figure 3. In Figure 2 Inlet BC corresponds to the exit of the last stage of the axial compressor, Outlet BC corresponds to the entrance of the turbine, Inlet and Outlet BTM identify the two junctions of the burner transfer matrix of Eq.(8).

Transfer matrix is applied removing every burner, so that the upstream port of each matrix is the exit from the plenum and the downstream is the inlet of the combustion chamber (see

Figure 2), following the criteria discussed in Ref.[27]. Operating conditions are taken from experimental data and from RANS simulations of the Ansaldo combustor [24]. As previously described, a spatial distribution of the temperature is defined using data coming from RANS simulations, so that the eigenvalue problem is solved considering the actual temperatures into the combustion chamber with a correct definition of the flame shape, Figure 4.

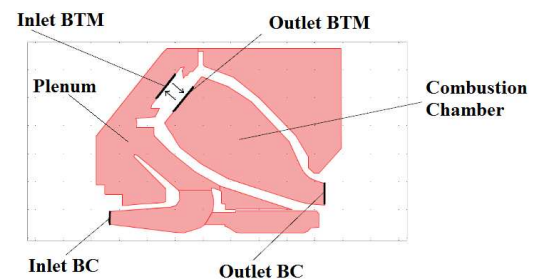


**Figure 2.** Computational domain and boundary conditions of the annular combustion chamber by Ansaldo Energia.

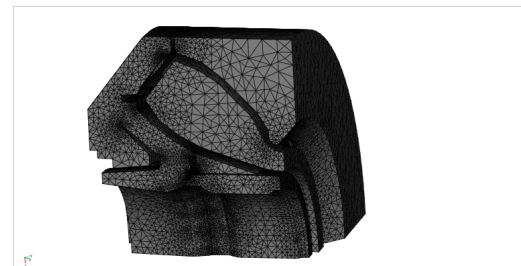


**Figure 3.** Computational grid of the annular combustion chamber.

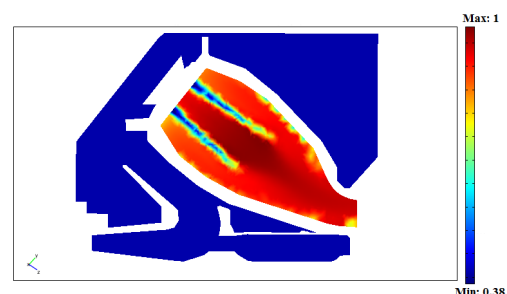


**Figure 4.** Temperature field from RANS simulation. The values are normalized against the maximum corresponding value.

Figure 5 shows the flame front inside the combustion chamber as it is captured by a RANS simulation. Flame front is clearly shown and the *Rate of Reaction* has zero value outside the flame. For the time delay distribution a certain number of particles is used and the procedure previously described has been followed. The time delay is considered non-zero only in the areas where the values of heat release are significant, as shown in Figure 6.

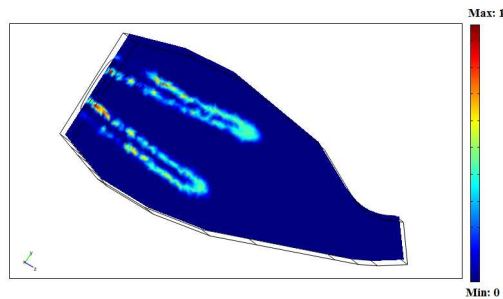


**Figure 5.** Normalized reaction rate distributions from RANS simulation.

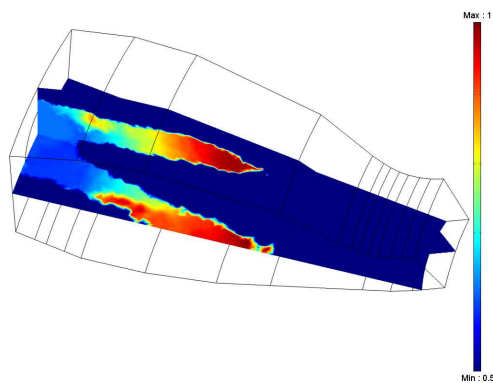


**Figure 6.** Normalized time delay distributions from RANS simulations.

#### 4.1 Analysis of Acoustic Modes Without Flame Fluctuations

The first 16 modes are searched for, when heat release fluctuations are not considered. A more detailed analysis of these 16 modes can be found in Ref. [27], where there are images of the acoustic pressure shape for each of them. For the sake of simplicity, only the mode shapes of two modes are shown: Mode 4 and Mode 13, which are azimuthal modes, but with different wave

index, involving both the plenum and the combustion chamber, Figure 7.

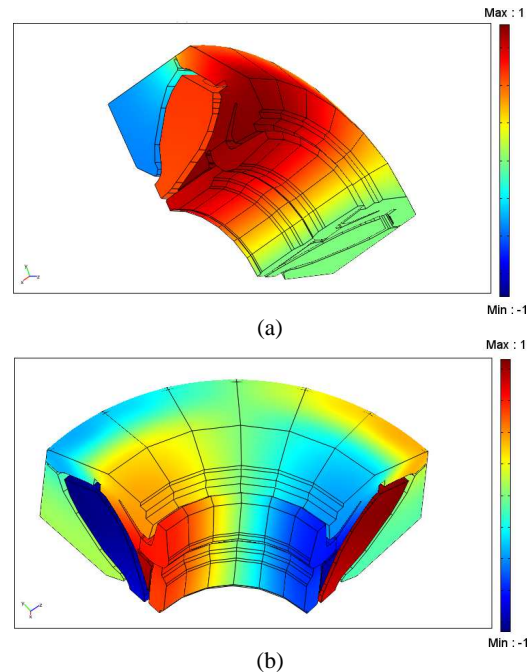


**Figure 7.** (a) Mode 4, azimuthal waveform  $n=1$ . (b) Mode 13, azimuthal waveform  $n=2$ .

#### 4.1 Analysis of Acoustic Modes With Flame Fluctuations

An investigation concerning the influence of the time delay  $\tau$  on the complex eigenfrequencies is carried out and the results are shown in Figure 8. For each mode five different eigenfrequencies are detected: four of them are referred to the case of a constant time delay in the flame model, Eq.(9), and one is referred to the case of spatial distribution of the time delay, as shown in Figure 6. The intensity index  $\kappa$  in the flame model is set to be equal to 1 in all the cases.

Figure 8 shows the influence of the time delay  $\tau$  on frequency and growth rate. Modes 11, 12 and 16 have mode shapes confined in a very small corner of the plenum, at a very small lengthscale, and they are asymptotically stable, so, for the sake of simplicity, they are not shown in Figure 8. Modes 1, 2, 5, 8, 14 and 15 are axial or azimuthal modes, whose mode shapes are located only in the plenum, and they are marginally stable, since not strongly influenced

by the variations of the time delay. On the other hand, variations in  $\tau$  determine large changes both in the frequency and in the growth rate for some modes, such as Modes 3, 4, 6 and 13: except for Mode 3, these all display an unstable condition for a strict range of  $\tau$ . Modes 4, 7, 9 and 10 have modeshapes located both in the plenum and in the combustion chamber and they experience an influence from  $\tau$  less than that experienced by Modes 3, 6 and 13 as previously explained.

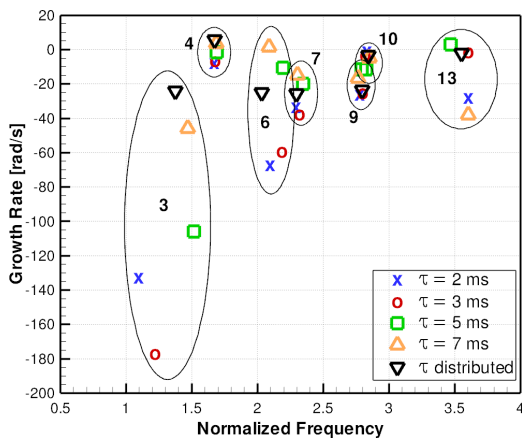


**Figure 8.** Combustion chamber modes for different values of  $\tau$  with the spatially distributed flame, Eq.(9).

The influence of the time delay  $\tau$  and of the intensity index  $\kappa$  on the stability is finally examined. To this purpose, for the sake of clarity, only Mode 13 is examined, since all the others show similar behavior.  $\tau$  moves from 1 to 9 ms, while  $\kappa$  moves from 0.5 to 1.5: there is a passage from a stable to an unstable condition for different values of the time delay. Increasing the intensity index  $\kappa$ , there is an increase in the intensity of the heat release inside the combustion chamber. As a consequence, the amplitude of the acoustic oscillations increases and the passage to an unstable condition is more likely to happen. Looking to Figure 9, increasing the intensity index  $\kappa$ , if the condition is unstable, the growth rate further increases. If the condition is stable, increasing the intensity index  $\kappa$ , the growth rate decreases.

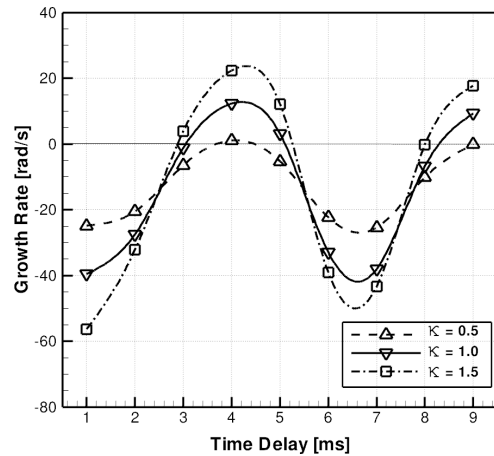


**Figure 9.** Mode 13 patterns for different values of  $\kappa$ ,

$$\text{Eq.} \left( \frac{q'(\mathbf{x})}{\bar{q}(\mathbf{x})} = -\kappa \frac{u_i'(t - \tau(\mathbf{x}))}{\bar{u}_i} \right) \quad (9).$$

## 5. Conclusions

This work demonstrates the COMSOL ability to import file data from other software and to correctly manage them. Additionally, COMSOL is able to treat complex geometries and to perform a thermoacoustic analysis. The complex eigenfrequencies of an industrial annular combustion chamber are detected and the influence of the flame parameters on the system stability is investigated, providing interesting information to designers and experimentalists.

## 8. References

- [1] H.J. Merk, "Analysis of Heat-Driven Oscillations of Gas Flows. General Considerations", *Applied Science Research*, pp.317-356, 1956.
- [2] T. Liewen, "Modeling Premixed Combustion-Acoustic Wave Interactions: A Review", *Journal of Propulsion and Power*, **19** (5), pp.765-781, 2003.
- [3] F. Culick, "Unsteady Motions in Combustion Chambers for Propulsion Systems", *RTO AGARDograph*, AG-AVT-039, 2006.
- [4] G.J. Bloxside, A.P. Dowling and P.J. Langhorne, "Reheat Buzz: an Acoustically Coupled Combustion Instability", *Journal of Fluid Mechanics*, **193**, pp.445-473, 1988.
- [5] A.P. Dowling, "The Calculation of Thermoacoustic Oscillations", *Journal of Sound and Vibration*, **180** (4), pp.557-581, 1995.
- [6] W. Polifke, C.O. Paschereit and T. Sattelmayer, "A Universally Applicable Stability Criterion for Complex Thermoacoustic Systems", *18th*

- Deutsch-Niederländischer Flammentag, VDI Bericht 1313*, pp.455-460, Delft, NL, 1997. M. Shell. (2002) IEEEtran homepage on CTAN.
- [7] B. Schuermans, V. Bellucci and C.O. Paschereit, "Thermoacoustic Modelling and Control of Multi Burner Combustion Systems", *ASME Paper*, GT2003-38688, 2003.
- [8] L. Selle, G. Lartigue, T. Poinsot, R. Koch, K.-U. Schildmacher, W. Krebs, B. Prade, P. Kaufmann and D. Veynante, "Compressible Large Eddy Simulation of Turbulent Combustion in Complex Geometry on Unstructured Meshes", *Combustion and Flame*, **137**, pp.489-505, 2004.
- [9] L. Benoit, "Prédictions des instabilités thermoacoustiques dans les turbines à gaz", *Ph.D. Thesis*, Université Montpellier II, 2005.
- [10] A. Giauque, L. Selle, T. Poinsot, H. Buechner, P. Kaufmann and W. Krebs, "System Identification of a Large-Scale Swirled Partially Premixed Combustor Using LES and Measurements", *Journal of Turbulence*, **6** (21), pp.1-20, 2005.
- [11] G. Staffelbach, L.Y.M. Gicquel, G. Boudier and T. Poinsot, "Large Eddy Simulation of Self Excited Azimuthal Modes in Annular Combustors", *Proceedings of the Combustion Institute*, **32**, pp.2909-2916, 2009.
- [12] C. Pankiewitz and T. Sattelmayer, "Time Domain Simulation of Combustion Instability", *ASME paper*, GT-2002-30063, 2002.
- [13] F. Nicoud, L. Benoit, C. Sensiau and T. Poinsot, "Acoustic Modes in Combustors with Complex Impedances and Multidimensional Active Flames", *AIAA Journal*, **45** (2), pp.426-441, 2007.
- [14] S.M. Camporeale, B. Fortunato and G. Campa, "A Finite Element Method for Three-Dimensional Analysis of Thermoacoustic Combustion Instability", *Journal of Engineering for Gas Turbine and Power*, **133** (1), 011506, 2011.
- [15] G. Campa and S.M. Camporeale, "A Novel FEM Method for Predicting Thermoacoustic Combustion Instability", *European COMSOL Conference*, 2009.
- [16] G. Campa and S.M. Camporeale, "Application of Transfer Matrix Method in Acoustics", *European COMSOL Conference*, 2010.
- [17] A.P. Dowling, "The Calculation of Thermoacoustic Oscillations", *Journal of Sound and Vibration*, **180** (4), pp.557-581, 1995.
- [18] A.P. Dowling and S.R. Stow, "Acoustic Analysis of Gas Turbine Combustors", *Journal of Propulsion and Power*, **19** (5), October 2003, pp.751-765.
- [19] R. Lehoucq and D. Sorensen, "Arpack: Solution of Large Scale Eigenvalue Problems with Implicitly Restarted Arnoldi Methods", [www.caam.rice.edu/software/arpack](http://www.caam.rice.edu/software/arpack). *User's Guide*.
- [20] D. Fanaca, P.R. Alemela, F. Ettner, C. Hirsch, T. Sattelmayer and B. Schuermans, "Determination and Comparison of the Dynamic Characteristics of a Perfectly Premixed Flame in Both Single and Annular Combustion Chamber", *ASME paper*, GT2008-50781.
- [21] P.R. Alemela, D. Fanaca, F. Ettner, C. Hirsch, T. Sattelmayer and B. Schuermans, "Flame Transfer Matrices of a Premixed Flame and a Global Check with Modeling and Experiments", *ASME paper*, GT2008-50111.
- [22] W. Krebs, P. Flohr, B. Prade and S. Hoffmann, "Thermoacoustic Stability Chart for High Intensity Gas Turbine Combustion Systems", *Combustion Science and Technology*, **174** (7), pp.99-128, 2002.
- [23] C.O. Paschereit, B. Schuermans, V. Bellucci and P. Flohr, "Implementation of Instability Prediction in Design: ALSTOM Approaches", *Chapter 15 in: Combustion Instabilities in Gas Turbine Engines*, T.C. Lieuwen and V. Yang eds, *Progress in Astronautics and Aeronautics*, **210**, pp.445-481, 2005.
- [24] D. Zito, F. Bonzani, C. Piana and A. Chiarioni, "Design Validation on Pressurized Test Rig of Upgraded Velonox Combustion System for F-Class Engine", *ASME paper*, GT2010-22256, 2010.
- [25] G. Waltz, W. Krebs, S. Hoffman and H. Judith, "Detailed Analysis of the Acoustic Mode Shapes of an Annular Combustion Chamber", *Journal of Engineering for Gas Turbine and Power*, **124**, January 2002.
- [26] A. Forte, S. Camporeale, B. Fortunato, F. Di Bisceglie and M. Mastrovito, "Effect of Burner and Resonator Impedances on the Acoustic Behaviour of Annular Combustion Chamber", *ASME paper*, GT2006-90423.
- [27] G. Campa, S.M. Camporeale, A. Guaus, J. Favier, M. Bargiacchi, A. Bottaro, E. Cosatto and G. Mori, "A Quantitative Comparison between a Low Order Model and a 3D FEM Code for the Study of Thermoacoustic Combustion Instability", *ASME paper*, GT2011-45969.

## 9. Acknowledgements

The work shown in this paper has been conducted as part of a joint research program supported by Ansaldo Energia. The authors gratefully acknowledge Giulio Mori and Federico Bonzani from Ansaldo Energia for their support throughout the whole project and for giving access to the industrial data. Additionally the authors gratefully acknowledge Aldo Chiarioni from Ansaldo Energia for his support in the interpretation of the RANS data of the Ansaldo Energia combustion chamber numerical simulation.